

Skeletocutins A-L: Antibacterial Agents from the Kenyan Wood-Inhabiting Basidiomycete, *Skeletocutis* sp.

Clara Chepkirui,^{†,^} Tian Cheng,^{†,^} Winnie Chemutai Sum,[‡] Josphat Clement Matasyoh,[§] Cony Decock,[⊥] Dimas F. Pradiya,^{||,#,∇} Kathrin Wittstein,[†] Eike Steinmann,^{||,#} and Marc Stadler^{*,†,Ⓛ}

[†]Department of Microbial Drugs, Helmholtz Centre for Infection Research (HZI), German Centre for Infection Research (DZIF), Partner Site Hannover/Braunschweig, Inhoffenstrasse 7, 38124 Braunschweig, Germany

[‡]Department of Biochemistry, Egerton University, P.O. BOX 536, 20115 Njoro, Kenya

[§]Department of Chemistry, Faculty of Sciences, Egerton University, P.O. Box 536, 20115 Njoro, Kenya

[⊥]Mycothèque de l' Université Catholique de Louvain (BCCM/MUCL), Place Croix du Sud 3, B-1348 Louvain-la-Neuve, Belgium

^{||}Department of Molecular and Medical Virology, Ruhr-University Bochum, 44801 Bochum, Germany

[#]TWINCORE—Centre for Experimental and Clinical Infection Research (Institute of Experimental Virology) Hanover, Feodor-Lynen-Str. 7-9, 30625 Hannover, Germany

[∇]Research Center for Biotechnology, Indonesian Institute of Science, Jl. Raya Bogor KM 46, Cibinong 16911, Indonesia

S Supporting Information

ABSTRACT: Fermentation of the fungal strain *Skeletocutis* sp. originating from Mount Elgon Natural Reserve in Kenya, followed by bioassay guided fractionation led to the isolation of 12 previously undescribed metabolites named skeletocutins A-L (1–5 and 7–13) together with the known tyromycin A (6). Their structures were assigned by NMR spectroscopy complemented by HR-ESIMS. Compounds 1–6 and 11–13 exhibited selective activities against Gram-positive bacteria, while compound 10 weakly inhibited the formation of biofilm of *Staphylococcus aureus*. The isolated metabolites were also evaluated for inhibition of L-leucine aminopeptidase, since tyromycin A had previously been reported to possess such activities but only showed weak effects. Furthermore, all compounds were tested for antiviral activity against Hepatitis C virus (HCV), and compound 6 moderately inhibited HCV infectivity with an IC₅₀ of 6.6 μM.

KEYWORDS: *polyporaceae, secondary metabolites, basidiomycota, structure elucidation*

■ INTRODUCTION

Tropical rainforest ecosystems represent a treasure trove of biological heritage, and the vast majority of its biodiversity still remain unexploited. The constant chemical innovations that exist in these habitats may be driven by the active evolutionary race, making tropical species a rich source for new bioactive molecules.¹ Fungi represent a considerable proportion of the total biodiversity in these ecosystems, but the majority of the tropical fungi remain unstudied for production of bioactive secondary metabolites. We have recently started to explore Basidiomycota from Kenya's rain forests, Kakamega and Mount Elgon National Reserve and have already reported several novel bioactive secondary metabolites from new or rare species. Those include the calocerins and the new 9-oxo strobilurins from *Favolaschia calocera*, the antibiotic laxitextines from *Laxitextum incrustatum*, the biofilm inhibitors named microporenic acids from *Microporus* sp. and the triterpenes, laetiporins and aethiopilonones from *Laetiporus* sp. and *Fomitiporia aethiopica*, respectively.^{2–6} Two strains of *Sanghuangporus* were also evaluated, and numerous bioactive compounds were discovered in their cultures.^{7,8} The current study deals with another basidiomycete, *Skeletocutis* sp. (MUCL56074) and the identification and characterization of its bioactive secondary metabolites.

Skeletocutis is a genus of about 40 species in family Polyporaceae. Even though this genus has a worldwide distribution, most of its known species are distributed in the Northern Hemisphere.⁹ Like other polypores, species in this genus are known to be forest pathogens causing white rot in a diverse array of woody plants. Interestingly, some species have been reported to grow on the dead fruiting bodies of other polypores, giving indications to their mycophilic lifestyle. Those include *Skeletocutis brevispora* and *Skeletocutis chrysellia*, which were reported from dead basidiomes of *Phellinidium ferrugineofusum* and *Phellinus chrysoloma*, respectively.¹⁰ Phylogenetically, *Skeletocutis* is closely related to the genus *Tyromyces*, and in recent phylogenetic studies, the two genera clustered together in the “*Tyromyces* clade” on a branch lying outside of the core polyporoid clade.^{11–13}

Herein we report the isolation, structure elucidation and bioactivities of 12 new compounds that are the first secondary metabolites known from *Skeletocutis*, and for which we propose the trivial names skeletocutins A-L accordingly.

Received: April 27, 2019

Revised: July 9, 2019

Accepted: July 16, 2019

Published: July 16, 2019

MATERIAL AND METHODS

General Experimental Procedures. NMR spectra were recorded with Bruker 700 spectrometer with 5 mm TXI cryoprobe (^1H 700 MHz, ^{13}C 175 MHz, ^{15}N 71 MHz) and Bruker AV II-500 (^1H 500 MHz, ^{13}C 125 MHz) spectrometers. HR-ESIMS mass spectra were recorded with Agilent 1200 series HPLC-UV system (column 2.1 \times 50 mm, 1.7 μm , C18 Acquity UPLC BEH (waters), solvent A: H_2O + 0.1% formic acid; solvent B: AcCN + 0.1% formic acid, gradient: 5% B for 0.5 min increasing to 100% in 19.5 min and then maintaining 100% B for 5 min, flow rate 0.6 mL/min, UV-vis detection 200–600 nm combined with ESI-TOF-MS (Maxis, Bruker)) [scan range 100–2500 m/z , capillary voltage 4500 V, dry temperature 200 $^\circ\text{C}$]. UV spectra were recorded by using a Shimadzu UV-2450 UV-vis spectrophotometer.

Fungal Material. The fungal specimen was collected by Decock and Matasyoh from Mount Elgon National Reserve, located in the western part of Kenya (1 $^\circ$ 7'6" N, 34 $^\circ$ 31'30" E). Dried specimen and corresponding cultures were deposited at MUCL, Louvain-la-Neuve, Belgium, under the accession number MUCL 56074. The genus was determined by morphological studies and comparison of the internal transcribed spacer (ITS)-nrDNA sequences with those of other Basidiomycota deposited in GenBank.

For molecular phylogenetic studies, DNA was extracted by using the EZ-10 Spin Column Genomic DNA Miniprep kit (Bio Basic Canada Inc., Markham, Ontario, Canada) as described previously.^{14,17} Precellys 24 homogenizer (Bertin Technologies, France) was used for cell disruption at a speed of 6000 rpm for 2 \times 40 s. Standard primers ITS 1f and NL4 were used for amplification of the 5.8S/ITS nrDNA regions according to the protocol of Lambert et al.¹⁶

Small-Scale Fermentation. *Skeletocutis* sp. MUCL56074 was cultivated in 3 different liquid media: YMG 6.3, Q6 1/2 and ZM 1/2 (media compositions see Supporting Information). A well grown culture from a YMG agar plate (YMG supplemented with 1.5% agar, pH 6.3) was cut into small pieces using a cork borer (7 mm) and five pieces were inoculated in a 500 mL Erlenmeyer flask containing 200 mL of the three media. The cultures were incubated on a rotary shaker (140 rpm) at 24 $^\circ\text{C}$. The growth of the fungus was monitored by constantly checking the amount of free glucose using Medi-test Glucose (Macherey-Nagel). The fermentation was terminated 2 days after glucose depletion.¹⁷

Scale-up of Fermentation. LC-MS dereplication was carried out by comparing the masses of the detected peaks and their molecular formula obtained from HRMS data with those in the Dictionary of natural products (<http://dnp.chemnetbase.com>). Several new compounds in the three media screened were detected in both the extracts from mycelia and supernatants. Preliminary LC-MS results indicated that similar metabolites were produced in all the three media but YMG medium produced the highest amount of metabolites, this medium was used in the scale-up. A well-grown YMG agar plate of mycelial culture was cut into small pieces using 7 mm cork border and five pieces inoculated into 500 mL sterile flasks containing 200 mL (25 flasks).

Preparation of the Extracts. Supernatant and biomass from small scale fermentation were separated by filtration. The supernatant was extracted with equal amount of ethyl acetate and filtered through anhydrous sodium sulfate. The resulting ethyl acetate extract was evaporated to dryness by means of rotary evaporator. The mycelia were extracted with 200 mL of acetone in ultrasonic bath for 30 min, filtered, and the filtrate evaporated. The remaining water phase was mixed with equal amount of distilled water, extracted with equal amount of ethyl acetate, and filtered through anhydrous sodium sulfate and dried by evaporator.

The mycelia and supernatant from the large scale fermentation were separated via vacuum filtration. The mycelia were ultrasonicated for 30 min with 4 \times 500 mL of acetone. The extracts were combined and evaporated and the remaining water phase was suspended in 200 mL distilled water and extracted 3 times with 500 mL ethyl acetate. The organic layer was filtered and evaporated to dryness, leaving brown solid extract (610.2 mg). 5% Amberlite XAD-16N adsorbent

(Rohm & Haas Deutschland GmbH, Frankfurt am Main, Germany) was added to the supernatant and shook overnight. The Amberlite resin was then filtered and eluted with 4 \times 500 mL of acetone. The resulting extract was evaporated and the remaining water phase was extracted three times with equal amount of ethyl acetate. The organic phase was dried by to afford 5.2 g of extract.

Isolation of Compounds 1–13. The extracts from mycelia and supernatant were combined and filtered using an SPME Strata-X 33 u Polymeric RP cartridge (Phenomenex, Inc., Aschaffenburg, Germany). The extract was then fractionated by preparative reverse phase liquid chromatography (PLC 2020, Gilson, Middleton, USA), using VP Nucleodur 100-5 C-18 ec column (25 \times 40 mm, 7 μm : Macherey-Nagel). Deionized water (Milli-Q, Millipore, Schwalbach, Germany) with 0.05% TFA (solvent A) and acetonitrile with 0.05% TFA (solvent B) were used as mobile phase. Elution gradient: 50% solvent B increased to 100% in 60 min and finally isocratic conditions at 100% solvent B for 5 min. The flow rate was 40 mL/min and UV detection was carried out at 210, 254, and 350 nm. A total of 22 fractions were collected according to the observed peaks (F1–F22). Detailed description of the methods can be found in the SI.

Antimicrobial Assays. Compounds 1–13 were evaluated for antimicrobial activity (minimum inhibition concentrations, MIC) in serial dilution assays against several test microorganisms (Table S) according to our previous research.^{14,15} The assays were conducted in 96-well plates in Mueller-Hinton broth (MHB) media for bacteria and YMG media for filamentous fungi and yeasts.

Cytotoxicity Assays. Compounds 1–13 were evaluated in the cytotoxicity assay against mouse fibroblasts (L929) and HeLa (KB3.1) cell lines as described previously.¹⁷

Biofilm Inhibition Assay. *Staphylococcus aureus* DSM1104 was grown overnight in casein-peptone soymeal-peptone (CASO) medium containing 4% glucose with PH7.0. The *S. aureus* cell concentration was adjusted to match the turbidity of 0.5 McFarland standard. The assay was performed in 96-well flat bottom plates (Falcon Microplates, U.S.A.) as previously described.¹⁸ Methanol was used as negative control; all experiments were carried out in triplicates and cytochalasin B was used as a standard (cf. Yuyama et al.¹⁹)

Nematicidal Assay. The nematicidal activity against *Caenorhabditis elegans* was performed in 24-well microtiter plates as previously described.²⁰ Ivermectin and methanol were used as positive and negative control, respectively. The results were expressed as LD₉₀.

Leucine Aminopeptidases Inhibition Assays. Hydrolysis of *L*-leucine-7-amido-4-methylcoumarin (*L*-Leu-AMC) by the surface bound aminopeptidases of HeLa (KB3.1) cell lines was evaluated according to the method described by Weber et al.²¹ with slight modifications. KB3.1 cells were grown as monolayer cultures in Dulbecco's Modified Eagle (DMEM) medium containing 10% of fetal calf serum at 37 $^\circ\text{C}$ in 24-well multidishes. After 3 days the confluent monolayers were washed twice with phosphate buffered saline (PBS) and the reaction mixture (450 μL Hank's buffer PH 7.2 containing 50 μM and 100 μM substrate *L*-Leu-AMC, and compounds dissolved in 50 μL DMSO) was added. After 30 min of incubation at 23 $^\circ\text{C}$, 1 mL of cold 0.2 M glycine-buffer PH 10.5 was added. The amount of hydrolyzed 7-amino-4-methylcoumarin (AMC) was determined in a fluorescence spectrophotometer (excitation/emission: 365/440 nm; Tecan Infinite M200 PRO). Bestatin²² and DMSO were used as positive control and negative control, respectively.

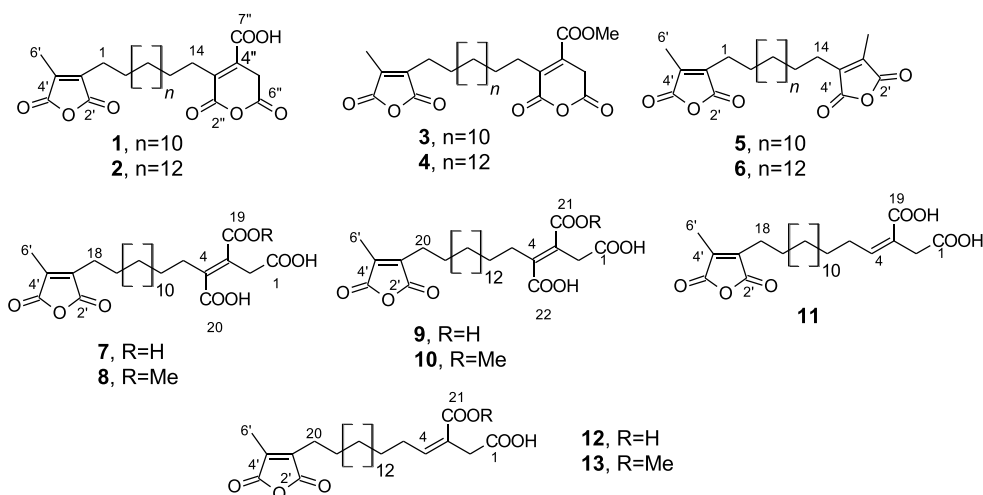
Inhibitory Effects on HCV Infectivity. Compounds 1–13 were tested for antiviral activity against Hepatitis C virus (HVC) as previously described.^{23,24} Detailed information can be found in the SI.

RESULTS AND DISCUSSION

As described in the Experimental section, the strain MUCL56074 was assigned to the genus *Skeletocutis* by morphological studies and sequencing of the rDNA (5.8S gene region and ITS). The BLAST result from GenBank confirmed the identity of this fungus to genus *Skeletocutis* in the Polyporaceae family. The closest hit was the DNA sequence with GenBank acc no KY953026.1 (*Skeletocutis*

Table 1. NMR Data (^1H 500 MHz and ^{13}C 125 MHz) in CDCl_3 for **1** and **2** and (^1H 500 MHz and ^{13}C 125 MHz) in $\text{Acetone-}d_6$ for **3** and **4**

no.	1		2		3		4	
	^{13}C	$^1\text{H}/\text{HSQC}$	^{13}C	$^1\text{H}/\text{HSQC}$	^{13}C	$^1\text{H}/\text{HSQC}$	^{13}C	$^1\text{H}/\text{HSQC}$
1	24.4, CH_2	2.46 (t), $J = 7.78$ Hz	24.4, CH_2	2.45 (t), $J = 7.78$ Hz	24.8, CH_2	2.50 (t), $J = 7.63$ Hz	24.1, CH_2	2.50 (t), $J = 7.48$ Hz
2	27.5, CH_2	1.60 (m)	27.6, CH_2	1.59 (m)	28.3, CH_2	1.60 (m)	28.2, CH_2	1.60 (m)
3–12/ 3–14	29.4–29.6, CH_2	1.26–1.32 (m)	29.1–29.9, CH_2	1.26–1.32 (m)	29.3–30.3, CH_2	1.28–1.36 (m)	29.4–30.3, CH_2	1.28–1.34 (m)
13/15	27.5, CH_2	1.62 (m)	27.6, CH_2	1.59 (m)	28.3, CH_2	1.61 (m)	28.3, CH_2	1.61 (m)
14/16	24.9, CH_2	2.50 (t), $J = 7.63$ Hz	27.6, CH_2	24.9 (t), $J = 7.63$ Hz	25.2, CH_2	2.57 (t), $J = 7.63$ Hz	25.2, CH_2	2.56 (t), $J = 7.78$ Hz
2'	165.9, C		165.9, C		167.2, C		167.2, C	
3'	144.8, C		144.8, C		145.0, C		145.0, C	
4'	140.5, C		140.4, C		141.8, C		141.8, C	
5'	166.3, C		166.3, C		167.4, C		167.4, C	
6'	9.5, CH_3	2.08 (s)	9.5, CH_3	2.07 (s)	9.6, CH_3	2.08 (s)	9.6, CH_3	2.08 (s)
2''	165.1, C		165.9, C		166.7, C		166.7, C	
3''	148.0, C		148.0, C		148.0, C		148.0, C	
4''	135.6, C		135.6, C		137.9, C		137.9, C	
5''	29.0, CH_2	3.57 (s)	29.1, CH_2	3.57 (s)	39.9, CH_2	3.68 (s)	30.1, CH_2	3.68 (s)
6''	165.1, C		165.9, C		166.4, C		166.4, C	
7''	171.5, C		171.3, C		169.0, C		169.1, C	
					52.6, OCH_3	3.7 (s)	52.9, OCH_3	3.7 (s)

**Figure 1.** Chemical structures of compounds **1**–**12**.

nivea) with 96.99% identity (see [Figure S106](#), Supporting Information), from which no metabolites had hitherto been reported.

The extracts from small scale fermentation of *Skeletocutis* sp. (strain MUCL 56074) exhibited good antibacterial activity (4.68 $\mu\text{g}/\text{mL}$) against *Bacillus subtilis*. Moreover, analyses of the secondary metabolite profiles by HPLC-MS pointed toward the presence of several hitherto unknown compounds. Therefore, extensive chromatographic studies of the extract as described in the Experimental Section were conducted and finally led to the isolation of 12 new compounds named skelotocutins A–L. Their characteristics are reported further below.

Compound **1** (skelotocutin A) with the molecular formula $\text{C}_{25}\text{H}_{34}\text{O}_8$ and nine degrees of unsaturation deduced from the HR-ESIMS spectrum was isolated as a white solid. The ^{13}C NMR spectroscopic data of **1** ([Table 1](#)) revealed the presence of 25 carbon signals, which could further be classified into one

methyl carbon, 15 methylene carbons and nine nonprotonated carbons (including five attached to heteroatoms) in the DEPT NMR spectrum. The HMBC correlations of $\text{H}_3\text{-}6'$ (δ 2.08) to $\text{C-}3'/\text{C-}4'/\text{C-}5'$ and $\text{H}_2\text{-}1$ to $\text{C-}2'/\text{C-}3'/\text{C-}4'$ confirmed the maleic anhydride moiety in the molecule. The presence of the glutaric anhydride moiety was revealed by HMBC correlations of $\text{H}_2\text{-}14$ (δ 2.50) to $\text{C-}2''/\text{C-}3''/\text{C-}4''$ and $\text{H}_2\text{-}5''$ (δ 3.57) to $\text{C-}3''/\text{C-}4''/\text{C-}6''$. Further, HMBC correlations of $\text{H-}5''$ to $\text{C-}7''$ confirmed the position of the $\text{C-}7''$ carboxylic acid substituent. COSY correlations of $\text{H}_2\text{-}1$ triplet (δ 2.46) to $\text{H}_2\text{-}2$ (δ 1.60) and $\text{H}_2\text{-}13$ (δ 1.62) to $\text{H}_2\text{-}14$ triplet (δ 2.50) were also observed. A multiplet resonating between (δ 1.26–1.32) was attributed to the remaining ten methylene groups of the tetradecamethylene chain in the molecule. This was further confirmed by the integration of the multiplet, which gave an integral value of 20, confirming the 20 methylene protons or C-3 to C-12. The connection of the tetradecamethylene chain to the maleic and glutaric anhydride moieties was confirmed by

HMBC correlations of H₂-1/H₂-2 to C-3' and H₂-13/H₂-14 to C-3'', respectively. Therefore, the structure of **1** was unambiguously concluded to be 5''-[14-(4'-methyl-2,5-dioxo-2,5-dihydrofuran-3-yl)tetradecyl]-2'',6''-dioxo-2'',6''-dihydropyran-4''-carboxylic acid (Figure 1).

Compound **2**, which had the molecular formula C₂₇H₃₈O₈ derived from HR-ESIMS data, was isolated as white solid. 1D and 2D NMR data of **2** pointed to a similar structure as **1** with the difference being the size of the carbon chain in the molecule. The multiplet occurring at δ 1.26–1.32 for the methylene groups (C-3-C-14) in **2** gave an integral value of 24 indicating a hexadecamethylene chain in the molecule instead of the tetradecamethylene chain elucidated for compound **1**. This was further supported by the fact that the two molecules mass difference was 28, which is equivalent to the mass of two methylene groups. The structure of **2** was therefore concluded to be 5''-[16-(4'-methyl-2',5'-dioxo-2',5'-dihydrofuran-3'-yl)-tetradecyl]-2'',6''-dioxo-2'',6''-dihydropyran-4''-carboxylic acid that we propose the trivial name skeletocutin B.

Compound **3** (skeletocutin C) with the molecular formula C₂₆H₃₆O₈ and 9 degrees of unsaturation and compound **4** with molecular formula C₂₈H₄₀O₈ and 9 degrees of unsaturation were obtained as yellow solid and white solid, respectively. Analysis of the ¹³C NMR spectra of **2** revealed a structure closely related to that of **1** with the difference being methoxy group signal occurring at δ 52.6. The methoxy group proton (δ 3.70) showed HMBC correlations to C-7'' (δ 169.0). Similarly, for compound **4** (skeletocutin D), the 1D and 2D NMR data indicated a similar structure as **2** with the difference being a methoxy group (δ 52.9) whose proton (δ 3.70) showed a HMBC correlation to C-7'' (δ 169.1).

Compound **5** (skeletocutin E), which was obtained as yellow oil, had the molecular formula C₂₄H₃₄O₆ and eight degrees of unsaturation. The ¹³C NMR spectrum of **5** showed only 12 signals which indicates that the compound consisted of two identical halves. A methyl singlet resonance at δ 2.07 (H₃-6') along with methylene groups triplet and quintet occurring at δ 2.45 (H₂-1/H₂-14) and δ 1.57 (H₂-2/H₂-13) respectively were observed in the ¹H NMR spectrum (Table 2). HMBC correlations of the C-6' methyl group proton (δ 2.07) to C-3'/C-4'/C-5' and H₂-1/H₂-14 to C-2'/C-3'/C-4' confirmed the maleic anhydride moiety in the molecule. Integration of the methyl singlet (H₃-6') gave an integral value of 6 confirming the presence of two maleic anhydride groups. The multiplet occurring between δ 1.26–1.32 was attributed to the

remaining ten methylene groups of carbon chain. The integral value of 20 obtained for this multiplet confirmed the chain length. Cross peaks in the HMBC spectrum between the H₂-1/H₂-14 and H₂-2/H₂-13 and C-3' confirmed the connection of the chain to the two maleic anhydride and therefore confirming the structure of **5** to be 1,14-bis [4'-methyl-2',5'-dioxo-3'-furyl] tetradecane. Compound **5** has been reported before as a product of chemical synthesis, but to the best of our knowledge it has never before been isolated from a natural source. The published MS data and ¹H and ¹³C NMR data reported for the synthetic product matched our own findings.²⁵

Compound **6** was isolated as white crystalline solid. The HR mass spectrum revealed the molecular formula to be C₂₆H₃₈O₆ with nine degrees of unsaturation. This compound was identified as tyromycin A by comparing its NMR and HR-MS data previously reported from *Tyromyces lacteus*, which belongs to the same family (Polyporaceae) as *Skeletocutis*.²¹ An efficient one-step synthesized of this compound using double radical decarboxylation has also been reported.²⁵

Compound **7** (skeletocutin F) with the molecular formula C₂₅H₃₆O₉ and eight degrees of unsaturation was isolated as yellow solid. Analysis of the 1D and 2D NMR data of **7** (Table 3) indicated the presence of the maleic anhydride like in the other compounds described above. Further, the HMBC correlations of H₂-18 (δ 2.39) to C-2'/C-3'-C4' confirmed the linkage of this moiety to the 14-carbon chain in the molecule. The three carboxylic acid moieties for the tricarboxylic acid part of the molecule had resonance at δ 171.5 (C-1), 171.4 (C-19), and 170.2 (C-20) in the ¹³C NMR spectrum. Cross peaks in the HMBC spectrum were observed between H₂-2 and C-1/C-3/C-4/C-19. HMBC correlations of H₂-5 to C-3/C-4/C-20 confirmed the connection of the tricarboxylic acid moiety to the chain and the position of C-20. The COSY correlations of H₂-5 to H₂-6 and H₂-18 to H₂-17 were also recorded. The olefinic bond between C-3 and C-4 was assigned the *E* configuration due to the absence of cross peaks in the ROESY spectra between the C-2 and C-5 methylene protons. The integration of the multiplet signal at δ 1.23–1.30 indicated ten additional methylene groups and hence the compound was identified as 3*E*-18-(4'-methyl-2',5'-dioxo-2',5'-dihydrofuran-3'-yl) octadecane-1,2,3-tricarboxylic acid.

Compound **8** (skeletocutin G) with molecular formula C₂₆H₃₈O₉ and 8 degrees of unsaturation was isolated as white solid. The ¹³C NMR spectra of **8** revealed a structure closely related to that of **7** with the difference being methoxy group, indicated by a signal occurring at δ 52.8. The methoxy group proton (δ 3.74) showed HMBC correlations to C-19 (δ 171.8).

Compound **9** (skeletocutin H), which was designated the molecular formula C₂₇H₄₀O₉ from the HRMS data was obtained as white solid. The 1 and 2D NMR data indicated a similar structure as **7** with the difference being the size of the carbon chain. The multiplet occurring at δ 1.28–1.36 for the methylene groups C-7-C-18 gave an integral value of 24 indicating icosane-1,2,3-tricarboxylic acid in the molecule instead of the octadecane-1,2,3-tricarboxylic acid elucidated in compound **7**.

Compound **10** (skeletocutin I) with molecular formula C₂₈H₄₂O₉, 1 and 2D NMR data indicated a similar structure as **9** with the difference being a methoxy group (δ 52.5) whose proton (δ 3.74) showed HMBC correlation to C-21 (δ 170.6).

Table 2. NMR Data (¹H 500 MHz and ¹³C 125 MHz) in CDCl₃ for **5** and (¹H 500 MHz and ¹³C 125 MHz) in DMSO for **6**

no.	5		6	
	¹³ C/HSQC	¹ H	¹³ C/HSQC	¹ H
1/14/16	24.4, CH ₂	2.45 (t), J = 7.78 Hz	23.6, CH ₂	2.40 (t), J = 7.53 Hz
2/13/15	3, CH ₂	1.57 (p), J = 7.78 Hz	26.7, CH ₂	1.48 (p), J = 7.53 Hz
3–12/14	29.1–29.6, CH ₂	1.26–1.32 (m)	28.6–29.0, CH ₂	1.23–1.29 (m)
2'	165.9, C		166.2, C	
3'	144.8, C		143.4, C	
4'	140.4, C		140.8, C	
5'	166.3, C		166.4, C	
6'	9.5, CH ₃	2.08 (s)	9.2, CH ₃	1.99 (s)

Table 3. NMR Data (^1H 500 MHz and ^{13}C 125 MHz) in DMSO for **7** (^1H 500 MHz and ^{13}C 125 MHz) in Acetone- d_6 for **9** and (^1H 500 MHz and ^{13}C 125 MHz) in CDCl_3 for **8** and **10**

7		8		9		10			
no.	$^{13}\text{C}/\text{HSQC}$	^1H	$^{13}\text{C}/\text{HSQC}$	^1H	no.	$^{13}\text{C}/\text{HSQC}$	^1H	$^{13}\text{C}/\text{HSQC}$	^1H
1	171.5, C		170.7, C		1	171.9, C		172.3, C	
2	36.9, CH_2	3.30 (s)	36.5, CH_2	3.60 (s)	2	37.4, CH_2	3.56 (s)	36.5, CH_2	3.61 (s)
3	128.0, C		128.1, C		3	129.5, C		128.2, C	
4	143.5, C		145.8, C		4	144.9, C		145.9, C	
5	30.4, CH_2	2.53 (t), $J = 7.9$ Hz	31.5, CH_2	2.72 (t), $J = 7.93$ Hz	5	31.9, CH_2	2.70 (t), $J = 7.93$ Hz	31.5, CH_2	2.73 (t), $J = 7.78$ Hz
6	28.1, CH_2	1.36 (q), $J = 6.71$ Hz	28.7, CH_2	1.54 (m)	6	29.5, CH_2	1.52 (br p), $J = 7.50$ Hz	28.7, CH_2	1.53 (m)
7/16	28.6–29.0, CH_2	1.2–1.30 (m)	29.2–29.7, CH_2	1.26–1.36(m)	7/18	29.3–30.4, CH_2	1.28–1.36 (m)	29.2–29.6, CH_2	1.25–1.31 (m)
17	26.9, CH_2	1.48 (q), $J = 7.48$ Hz	27.6, CH_2	1.57 (m)	19	28.3, CH_2	1.59 (br p), $J = 7.48$ Hz	27.7, CH_2	1.57 (m)
18	23.6, CH_2	2.39, (s), $J = 7.48$ Hz	24.4, CH_2	2.45 (s), $J = 7.71$ Hz	20	24.8, CH_2	2.50, (s), $J = 7.63$ Hz	24.4, CH_2	2.46, (t), $J = 8.09$ Hz
19	171.4, C		171.8, C		21	169.0, C		171.6, C	
20	170.2, C		171.6, C		22	170.5, C		171.8, C	
2'	166.2, C		165.9, C		2'	167.2, C		165.9, C	
3'	143.5, C		144.8, C		3'	145.0, C		144.8, C	
4'	140.9, C		140.4, C		4'	141.8, C		140.5, C	
5'	166.4, C		166.3, C		5'	167.4, C		166.3, C	
6'	9.2, CH_3	1.99 (s)	9.5, CH_3	2.08 (s)	6'	9.6, CH_3	2.08 (s)	9.5, CH_3	2.08 (s)
			52.8, OCH_3	3.74 (s)				52.5, OCH_3	3.74 (s)

Table 4. NMR Data (^1H 500 MHz and ^{13}C 125 MHz) in CDCl_3 CDCl_3 for **11–13**

11			12			13			
no.	$^{13}\text{C}/\text{HSQC}$	^1H	no.	$^{13}\text{C}/\text{HSQC}$	^1H	$^{13}\text{C}/\text{HSQC}$	^1H	$^{13}\text{C}/\text{HSQC}$	^1H
1	176.3, C		1	177.2, C		171.2, C			
2	32.1, CH_2	3.37 (s)	2	32.1, CH_2	3.37 (s)	31.8, CH_2	3.36 (s)		
3	124.4, C		3	124.5, C		124.6, C			
4	148.9, CH	7.11 (t), $J = 7.48$ Hz	4	148.9, CH	7.12 (t), $J = 7.48$ Hz	148.8, CH	7.10 (t), $J = 7.63$ Hz		
5	29.2, CH_2	2.23 (q), $J = 7.48$ Hz	5	29.1, CH_2	2.22 (q), $J = 7.48$ Hz	28.7, CH_2	2.21 (q), $J = 7.63$ Hz		
6	28.3, CH_2	1.47 (p), $J = 7.48$ Hz	6	28.3, CH_2	1.47 (p), $J = 7.48$ Hz	28.3, CH_2	1.47 (p), $J = 7.63$ Hz		
7–16	29.2–29.6, CH_2	1.26–1.31 (m)	7–18	29.1–29.6, CH_2	1.26–1.31 (m)	29.4–2.6, CH_2	1.26–1.32(m)		
17	27.5, CH_2	1.58 (P), $J = 7.63$ Hz	19	27.5, CH_2	1.58 (p), $J = 7.55$ Hz	27.6, CH_2	1.58 (p), $J = 7.32$ Hz		
18	24.4, CH_2	2.46, (t), $J = 7.63$ Hz	20	24.4, CH_2	2.45, (t), $J = 7.55$ Hz	24.4, CH_2	2.45, (t), $J = 7.32$ Hz		
19	171.9, C		21	172.4, C		171.2, C			
2'	165.9, C		2'	165.9, C		165.9, C			
3'	144.8, C		3'	144.8, C		144.8, C			
4'	140.4, C		4'	140.4, C		140.4, C			
5'	166.3, C		5'	166.3, C		166.3, C			
6'	9.5, CH_3	2.07 (s)	6'	9.5, CH_3	2.07 (s)	9.5, CH_3	2.07 (s)		
						52.1, OCH_3	3.69 (s)		

Compound **11** (skeletalocutin J), which was assigned the molecular formula $\text{C}_{24}\text{H}_{36}\text{O}_7$ from the HRMS data, was isolated as white oil. Analysis of the 1D and 2D NMR data suggested a structure closely related to that of **7**, with the difference being the absence of the tricarboxylic acid moiety and the presence of a dicarboxylic acid moiety instead. HMBC correlations of H_2 -2 to C-1/C-3/C-4/C-19, H-4 to C-2/C-19/C-5/C-6 and H_2 -5 to C-3/C-4/C-6 were observed. Further, COSY correlations of H_2 -5 to H-4/ H_2 -6 were also recorded. The olefinic bond between C-4 and C-5 was assigned the *cis* configuration because of the small coupling constant of 7.48 Hz recorded. Therefore, the structure of **11** was concluded to be (3*Z*)-3-[6-(4'-methyl-2',5'-dioxo-2',5'-dihydrofuran-3'-yl)pentadecene]butanedioic acid.

Compound **12** (skeletalocutin K) which was isolated as yellow oil, had molecular formula $\text{C}_{26}\text{H}_{40}\text{O}_7$ deduced from the HR mass spectrum. The 1 and 2 D NMR data revealed a similar structure as **11** but the integration of the methylene groups' multiplet occurring between δ 1.26–1.31 gave an integral value of 24 suggesting a 16 carbon chain. Also, the mass difference between these two compounds is 28 i. e two methylene groups. Hence, the structure of **12** was unambiguously assigned as (3*Z*)-3-[6-(4'-methyl-2',5'-dioxo-2',5'-dihydrofuran-3'-yl)heptadecene]butanedioic acid (Table 4).

Compound **13** (skeletalocutin L), which was designated the molecular formula $\text{C}_{27}\text{H}_{42}\text{O}_7$ from the HRMS data was isolated as yellow oil. The 1D and 2 D NMR data indicated a similar structure as **12** with the difference being a methoxy group (δ

Table 5. Antimicrobial Activities of Compounds 1–13

organism	MIC ($\mu\text{g/mL}$)									
	1	2	3	4	5	6	11	12	13	ref
<i>Bacillus subtilis</i> DSM10	150	18.75	37.5	75	18.75	9.375	300		18.75	3.1 ^a
MRSA <i>Staphylococcus aureus</i> DSM11822	150	150	300	300	150	150	150	75	75	0.4 ^b
<i>Staphylococcus aureus</i> DSM346	37.5	300	150	150	37.5	150	150	37.5	18.75	6.7 ^c
<i>Micrococcus luteus</i> DSM20030	150				150	150		150	37.5	0.4 ^c

^aCiprofloxacin. ^bVancomycin. ^cOxytetracycline.

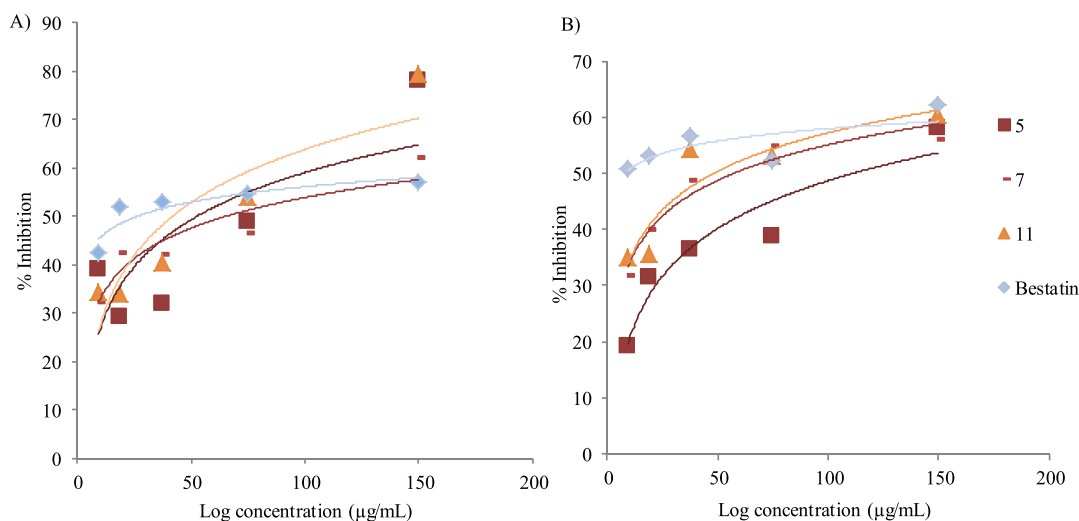


Figure 2. Inhibition of hydrolysis of leu-AMC (A) concentration of L -Leu-AMC: 100 μM and (B) concentration of L -Leu-AMC: 50 μM .

52.1). The protons of the methoxy group (δ 3.69) showed a HMBC correlation to C-21 (δ 171.2).

Biological Activity. Compounds 1–13 were evaluated for their antimicrobial activity against different organisms (Table 5). All tested compounds except for 7–10 showed moderate activity against *Bacillus subtilis*, *Staphylococcus aureus*, and *Micrococcus luteus* with compounds 1–3, 5–6, and 12–13 exhibiting the highest activity in the range of 9.38–37.5 $\mu\text{g/mL}$. Further, the compounds demonstrated weak activities against MRSA (methicillin resistant *Staphylococcus aureus*). Neither of the compounds showed any activity against the tested Gram negative bacteria (*Chromobacterium violaceum*, *Escherichia coli*, *Mycobacterium smegmatis*, and *Pseudomonas aeruginosa*) nor fungi (*Candida albicans*, *Candida tenuis*, *Mucor plumbeus*, and *Pichia anomala*).

All compounds were also tested for nematicidal activities against *Caenorhabditis elegans* and cytotoxicity against mouse fibroblast (L929) and HeLa (KB 3.1) cell lines but they did not show any significant activities in these assays at concentrations ≤ 100 $\mu\text{g/mL}$ and 37 $\mu\text{g/mL}$, respectively. Compounds that did not show any significant activity (i.e with MIC ≥ 150 $\mu\text{g/mL}$) against *S. aureus* were subjected to the biofilm inhibition assay against *S. aureus* biofilm. Only compound 10 inhibited the formation of the biofilm up to 86% at 256 $\mu\text{g/mL}$ and 28% at 150 $\mu\text{g/mL}$. Tyromycin A (6) was reported before as an inhibitor of leucine aminopeptidase in HeLa S3 cells,²¹ hence the novel analogues were also tested for inhibition of L -Leu-AMC hydrolysis in HeLa (KB 3.1) cells. Only compounds 5, 7, 11, and 13 were weakly active in this assay with IC₅₀ values in the range 72.3–92.5 and 78.3–118.4 $\mu\text{g/mL}$ when 100 and 50 μM of the substrate were used, respectively (Figure 2 and Table 6). Even though tyromycin A

Table 6. Inhibition of L -Leu-AMC by the Metabolites from *Skeletocutis* sp

compounds	IC ₅₀ ($\mu\text{g/mL}$)	
	substrate (100 μM)	substrate (50 μM)
5	84	118.4
7	92.5	89.7
11	72.3	78.3
13	88.7	113.9
bestatin	10.8	40.9

(6) was previously reported to be active in a similar assay against HeLa S3 cells with IC₅₀ values of 31 $\mu\text{g/mL}$ at 50 μM substrate concentration, an IC₅₀ value >150 $\mu\text{g/mL}$ for this compound was recorded on the HeLa (KB3.1) cells when tested in this study.

Furthermore, all of the compounds were tested for their antiviral activity against hepatitis C virus (HCV), which is one of the major causes of chronic liver disease, with 71 million people infected worldwide. Although curative medications are available for HCV, the majority of infected individuals do not having an access to treatment due to high cost of the treatment. In a cellular replication assay to evaluate antiviral activity against HCV in human liver cells (Figure 3), compound 6 strongly inhibited HCV infectivity at the initial concentration 40 μM while compounds 4 and 5 inhibited HCV with moderate activity. Compounds 1, 3 and 13 showed weak activity and the rest of compound were not active. All tested compounds except for 6 were found devoid of cytotoxicity on the liver cells. We therefore next evaluated the antiviral activity of 6 against HCV in a dose dependent manner. As depicted in Figure 3C, incubation of 6 for 3 days

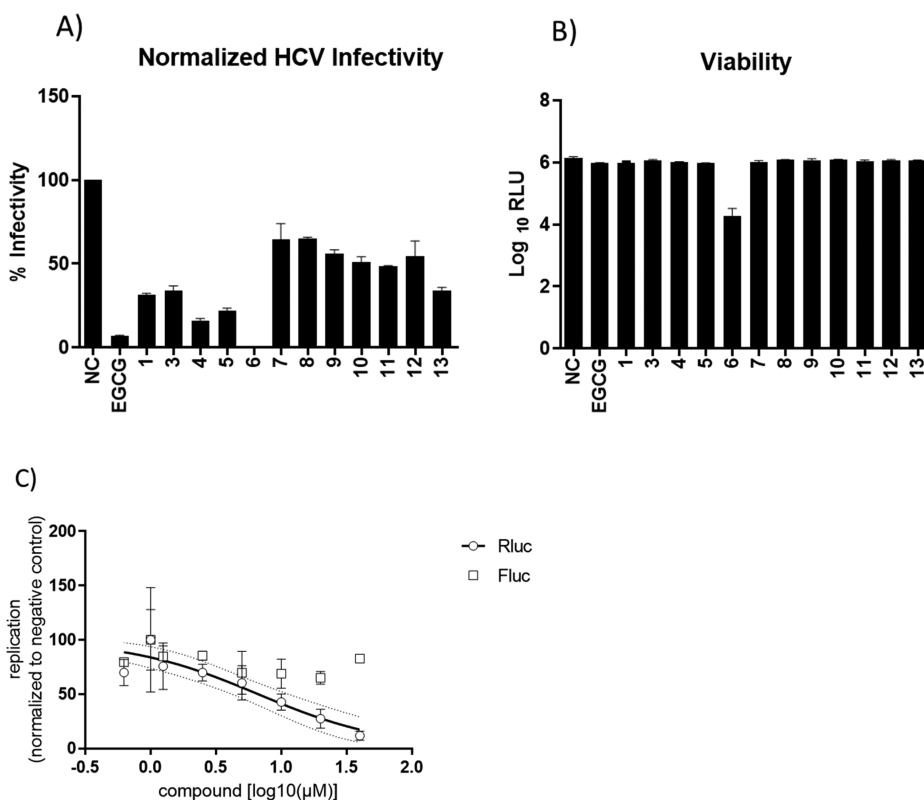


Figure 3. Antiviral activity of compound 1-13 against Hepatitis C virus (HCV). Huh-7.5 cells were inoculated with RLuc-Jc1 reporter viruses in the presence of the compounds. The inoculum was removed 4 h later and monolayers were washed three times with PBS and overlaid with fresh medium containing no inhibitors. Infected cells were lysed 3 days later, and reporter virus infection was determined by the *Renilla* luciferase activity (A). The cell viability was measured by determination of *Firefly* luciferase (B), which is stably expressed in the target cells. Dose-dependent inhibition of HCV infectivity was observed after treatment with compound 6 for 3 days (C).

resulted in a dose-dependent inhibition of HCV infectivity with a 50% inhibitory concentration (IC_{50}) of 6.6 μ M. The green tea molecule epigallocatechin gallate (EGCG) was used as positive control.²⁴

Skeletocutin A (1). White solid; UV (MeOH) $\lambda_{max}(\log \epsilon)$ 209 (4.54), 257 (3.02); ESIMS m/z 947 [2 M + Na]⁺, 485 [M + Na]⁺, 463 [M + H]⁺, 445 [M + H - H₂O]⁺; HRMS m/z 463.2330 [M + H]⁺ (calcd for C₂₅H₃₅O₈, 463.2331).

Skeletocutin B (2). White solid; UV (MeOH) $\lambda_{max}(\log \epsilon)$ 206 (4.54), 256 (3.02); ESIMS m/z 1003 [2 M + Na]⁺, 513 [M + Na]⁺, 491 [M + H]⁺, 473 [M + H - H₂O]⁺; HRMS m/z 491.2646 [M + H]⁺ (calcd for C₂₇H₃₉O₈, 491.2645).

Skeletocutin C (3). Yellow solid; UV (MeOH) $\lambda_{max}(\log \epsilon)$ 215 (4.65), 256 (3.17); ESIMS m/z 975 [2 M + Na]⁺, 499 [M + Na]⁺, 477 [M + H]⁺, 459 [M + H - H₂O]⁺; HRMS m/z 477.2470 [M + H]⁺ (calcd for C₂₆H₃₇O₈, 477.2488).

Skeletocutin D (4). White solid; UV (MeOH) $\lambda_{max}(\log \epsilon)$ 222 (4.39), 253 (3.61); ESIMS m/z 1031 [2 M + Na]⁺, 527 [M + Na]⁺, 505 [M + H]⁺, 487 [M + H - H₂O]⁺; HRMS m/z 505.2798 [M + H]⁺ (calcd for C₂₈H₄₁O₈, 505.2801).

Skeletocutin E (5). Yellow oil; UV (MeOH) $\lambda_{max}(\log \epsilon)$ 207 (4.39), 253 (3.65); ESIMS m/z 859 [2 M + Na]⁺, 441 [M + Na]⁺, 419 [M + H]⁺, 401 [M + H - H₂O]⁺; HRMS m/z 419.2429 [M + H]⁺ (calcd for C₂₄H₃₅O₆, 419.2433).

Tyromycin A (6). White crystalline solid; UV (MeOH) $\lambda_{max}(\log \epsilon)$ 214 (3.74), 256 (3.62); ESIMS m/z 915 [2 M + Na]⁺, 469 [M + Na]⁺, 447 [M + H]⁺, 429 [M + H - H₂O]⁺; HRMS m/z 447.2738 [M + H]⁺ (calcd for C₂₆H₃₉O₆, 447.2746).

Skeletocutin F (7). Yellow solid; UV (MeOH) $\lambda_{max}(\log \epsilon)$ 215 (4.48), 252 (3.08); ESIMS m/z 983 [2 M + Na]⁺, 503 [M + Na]⁺, 481 [M + H]⁺, 463 [M + H - H₂O]⁺; HRMS m/z 481.2422 [M + H]⁺ (calcd for C₂₅H₃₇O₉, 481.2437).

Skeletocutin G (8). White solid; UV (MeOH) $\lambda_{max}(\log \epsilon)$ 214 (4.20), 253 (4.33); ESIMS m/z 1011 [2 M + Na]⁺, 517 [M + Na]⁺, 495 [M + H]⁺, 477 [M + H - H₂O]⁺; HRMS m/z 495.2576 [M + H]⁺ (calcd for C₂₆H₃₉O₉, 495.2594).

Skeletocutin H (9). White solid; UV (MeOH) $\lambda_{max}(\log \epsilon)$ 227 (4.09), 256 (3.68); ESIMS m/z 1039 [2 M + Na]⁺, 531 [M + Na]⁺, 509 [M + H]⁺, 491 [M + H - H₂O]⁺; HRMS m/z 509.2746 [M + H]⁺ (calcd for C₂₇H₄₁O₉, 509.2750).

Skeletocutin I (10). White solid; UV (MeOH) $\lambda_{max}(\log \epsilon)$ 218 (4.28), 255 (3.40); ESIMS m/z 1067 [2 M + Na]⁺, 545 [M + Na]⁺, 523 [M + H]⁺, 505 [M + H - H₂O]⁺; HRMS m/z 523.2904 [M + H]⁺ (calcd for C₂₈H₄₃O₉, 523.2907).

Skeletocutin J (11). White oil; UV (MeOH) $\lambda_{max}(\log \epsilon)$ 218 (4.27), 256 (3.87); ESIMS m/z 895 [2 M + Na]⁺, 459 [M + Na]⁺, 437 [M + H]⁺, 419 [M + H - H₂O]⁺; HRMS m/z 437.2519 [M + H]⁺ (calcd for C₂₄H₃₇O₇, 437.2539).

Skeletocutin K (12). Yellow oil; UV (MeOH) $\lambda_{max}(\log \epsilon)$ 216 (4.505), 253 (4.02); ESIMS m/z 951 [2 M + Na]⁺, 487 [M + Na]⁺, 465 [M + H]⁺, 447 [M + H - H₂O]⁺; HRMS m/z 465.2850 [M + H]⁺ (calcd for C₂₆H₄₁O₇, 465.2852).

Skeletocutin L (13). Yellow oil; UV (MeOH) $\lambda_{max}(\log \epsilon)$ 218 (4.21), 259 (3.97); ESIMS m/z 979 [2 M + Na]⁺, 501 [M + Na]⁺, 479 [M + H]⁺, 461 [M + H - H₂O]⁺; HRMS m/z 479.2993 [M + H]⁺ (calcd for C₂₇H₄₃O₇, 479.3008).

■ ASSOCIATED CONTENT

Supporting Information

The Supporting Information is available free of charge on the ACS Publications website at DOI: 10.1021/acs.jafc.9b02598.

Experimental procedures, 1D and 2D NMR data, LCMS data, 5.8S/ITS DNA sequence of the producing organism (PDF)

■ AUTHOR INFORMATION

Corresponding Author

*Tel: +49-53161814240. Fax: +49-53161819499. E-mail: marc.stadler@helmholtz-hzi.de.

ORCID

Marc Stadler: 0000-0002-7284-8671

Author Contributions

^C.C. and T.C. contributed equally to this work.

Notes

The authors declare no competing financial interest.

■ ACKNOWLEDGMENTS

We are grateful to W. Collisi for conducting the cytotoxicity assays, C. Kakoschke for recording NMR data, and C. Schwager and E. Surges for recording HPLC-MS data. Financial support by the "ASAFEM" Project (Grant no. IC-070) under the ERAfrica Programme of the European Commission to C.D., J.C.M., and M.S. is gratefully acknowledged. Personal Ph.D. stipends from the German Academic Exchange Service (DAAD), the Kenya National Council for Science and Technology (NACOSTI), and the China Scholarship Council (CSC), to C.C., D.P., and T.C., respectively, are gratefully acknowledged.

■ REFERENCES

- (1) Sandargo, B.; Chepkirui, C.; Cheng, T.; Chaverra-Muñoz, L.; Thongbai, B.; Stadler, M.; Hüttel, S. Biological and chemical diversity go hand in hand: Basidiomycota as source of new pharmaceuticals and agrochemicals. *Biotechnol. Adv.* **2019**, S0734, 30011–30014, DOI: 10.1016/j.biotechadv.2019.01.011.
- (2) Chepkirui, C.; Richter, C.; Matasyoh, J. C.; Stadler, M. Monochlorinated calocerins A-D and 9-oxostrobilurin derivatives from the basidiomycete *Favolaschia calocera*. *Phytochemistry* **2016**, 132, 95–101.
- (3) Mudalungu, C. M.; Richter, C.; Wittstein, K.; Abdalla, M. A.; Matasyoh, J. C.; Stadler, M.; Süßmuth, R. D. Laxitextines A and B, cyathane xylosides from the tropical fungus *Laxitextum incrustatum*. *J. Nat. Prod.* **2016**, 79, 894–898.
- (4) Chepkirui, C.; Matasyoh, J. C.; Decock, C.; Stadler, M. Two cytotoxic triterpenes from cultures of a Kenyan *Laetiporus* sp. (Basidiomycota). *Phytochem. Lett.* **2017**, 20, 106–110.
- (5) Chepkirui, C.; Yuyama, K. T.; Wanga, L. A.; Decock, C.; Matasyoh, J. C.; Abraham, W.-R.; Stadler, M. Microporenic acids A-G, biofilm inhibitors, and antimicrobial agents from the basidiomycete *Microporus* species. *J. Nat. Prod.* **2018**, 81, 778–784.
- (6) Chepkirui, C.; Sum, W. C.; Cheng, T.; Matasyoh, J. C.; Decock, C.; Stadler, M. Aethiopinolones A-E, new pregnenolone type steroids from the East African basidiomycete *Fomitiporia aethiopica*. *Molecules* **2018**, 23, 369.
- (7) Cheng, T.; Chepkirui, C.; Decock, C.; Matasyoh, J. C.; Stadler, M. Sesquiterpenes from an Eastern African medicinal mushroom belonging to the genus *Sanguangporus*. *J. Nat. Prod.* **2019**, 82, 1283–1291.
- (8) Chepkirui, C.; Cheng, T.; Matasyoh, J. C.; Decock, C.; Stadler, M. An unprecedented spiro [furan-2,1'-indene]-3-one derivative and other nematocidal and antimicrobial metabolites from *Sanguangporus*

sp. (Hymenochaetaceae, Basidiomycota) collected in Kenya. *Phytochem. Lett.* **2018**, 25, 141–146.

(9) Cui, B.-K.; Dai, Y.-C. *Skeletocutis luteolus* sp. nov. from southern and eastern China. *Mycotaxon* **2008**, 104, 97–101.

(10) Ryvardeen, L.; Melo, I. Poroid fungi of Europe. *Synopsis Fungorum* **2017**, 37.

(11) Yao, Y.-J.; Pegler, D. N.; Chase, M. W. Application of ITS (nrDNA) sequences in the phylogenetic study of *Tyromyces* s.l. *Mycol. Res.* **1999**, 103, 219–229.

(12) Kim, S.-Y.; Park, S.-Y.; Jung, H.-S. Phylogenetic classification of *Antrrodia* and related genera based on ribosomal RNA internal transcribed spacer sequences. *J. Microbiol. Biotechnol.* **2001**, 11, 475–481.

(13) Floudas, D.; Hibbett, D. S. Revisiting the taxonomy of *Phanerochaete* (Polyporales, Basidiomycota) using a four gene dataset and extensive its sampling. *Fungal Biol.* **2015**, 119, 679–719.

(14) Richter, C.; Helaly, S. E.; Thongbai, B.; Hyde, K. D.; Stadler, M. Pyriatriatins A and B: pyridino-cyathane antibiotics from the basidiomycete *Cyathus cf. striatus*. *J. Nat. Prod.* **2016**, 79, 1684–1688.

(15) Wendt, L.; Sir, E. B.; Kuhnert, E.; Heitkämper, S.; Lambert, C.; Hladki, A. I.; Romero, A. I.; Luangsa-Ard, J. J.; Srikitkulchai, P.; Peršoh, D.; Stadler, M. Resurrection and emendation of the Hypoxylaceae, recognised from a multigene phylogeny of the Xylariales. *Mycol. Prog.* **2018**, 17, 115–154.

(16) Lambert, C.; Wendt, L.; Hladki, A. I.; Stadler, M.; Sir, E. B. *Hypomontagnella* (Hypoxylaceae): a new genus segregated from *Hypoxylon* by a polyphasic taxonomic approach. *Mycol. Prog.* **2019**, 18, 187–201.

(17) Kuhnert, E.; Surup, F.; Herrmann, J.; Huch, V.; Müller, R.; Stadler, M. Rickenyls A-E, antioxidative terphenyls from the fungus *Hypoxylon rickii* (Xylariaceae, Ascomycota). *Phytochemistry* **2015**, 118, 68–73.

(18) Yuyama, K. T.; Chepkirui, C.; Wendt, L.; Fortkamp, D.; Stadler, M.; Abraham, W.-R. Bioactive compounds produced by *Hypoxylon fragiforme* against *Staphylococcus aureus* biofilms. *Microorganisms* **2017**, 5, 80.

(19) Yuyama, K. T.; Wendt, L.; Surup, F.; Kretz, R.; Chepkirui, C.; Wittstein, K.; Boonlarppradab, C.; Wongkanoun, S.; Luangsa-Ard, J.; Stadler, M.; Abraham, W. R. Cytochalasins act as inhibitors of biofilm formation of *Staphylococcus aureus*. *Biomolecules* **2018**, 8, 129.

(20) Rupcic, Z.; Chepkirui, C.; Hernández-Restrepo, M.; Crous, P.; Luangsa-Ard, J.; Stadler, M. New nematocidal and antimicrobial secondary metabolites from a new species in the new genus, *Pseudobambusicola thailandica*. *Myckeys* **2018**, 33, 1–23.

(21) Weber, W.; Semar, M.; Anke, T.; Bross, M.; Steglich, W. Tyromycin A: A novel inhibitor of leucine and cysteine aminopeptidases from *Tyromyces lacteus*. *Planta Med.* **1992**, 58, 56–59.

(22) Mathé, G. Bestatin, an aminopeptidase inhibitor with a multi-pharmacological function. *Biomed. Pharmacother.* **1991**, 45, 49–54.

(23) Sandargo, B.; Michehl, M.; Praditya, D.; Steinmann, E.; Stadler, M.; Surup, F. Antiviral meroterpenoid rhodatin and sesquiterpenoids rhodocoranes A-E from the wrinkled peach mushroom. *Org. Lett.* **2019**, 21, 3286–3289.

(24) Ciesek, S.; von Hahn, T.; Colpitts, C. C.; Schang, L. M.; Friesland, M.; Steinmann, J.; Manns, M. P.; Ott, M.; Wedemeyer, H.; Meuleman, P.; Pietschmann, T. The green tea polyphenol, epigallocatechin-3-gallate, inhibits hepatitis C virus entry. *Hepatology* **2011**, 54, 1947–1955.

(25) Poigny, S.; Guyot, M.; Samadi, M. One-step synthesis of tyromycin A and analogues. *J. Org. Chem.* **1998**, 63, 1342–1343.